Structures 57 (2023) 105093

Contents lists available at ScienceDirect

Structures

journal homepage: www.elsevier.com/locate/structures

Seismic control of cross laminated timber (CLT) structure with shape memory alloy-based semi-active tuned mass damper (SMA-STMD)

Luyue Yan [a], Yi Li [a], Wen-Shao Chang [b], Haoyu Huang [c,*]

[a] Faculty of Architecture, Civil and Transportation Engineering, Beijing University of Technology, Beijing 100124, China
[b] Lincoln School of Architecture and the Built Environment, University of Lincoln, Lincoln LN6 7TS, UK
[c] School of Engineering, Newcastle University, Newcastle upon Tyne NE1 7RU, UK

ARTICLE INFO

Keywords:
Semi-active control
Cross laminated timber structure
Tuned mass damper
Shape memory alloy
Seismic control

ABSTRACT

Cross laminated timber (CLT) is becoming increasingly popular for constructing multiple-story buildings due to its alignment with Sustainable Development Goals of United Nations. However, such structures can be susceptible to excessive vibrations during earthquakes. While tuned mass dampers (TMDs) can be used to control these vibrations in CLT structures, their effectiveness can be reduced due to the lightweight nature of CLT and changes in its structural mass or deterioration of the wood. To address this issue, this paper proposes the use of shape memory alloy-based semi-active tuned mass dampers (SMA-STMDs) for controlling vibrations in CLT structures. This study includes the design and experimental testing of a full-scale, novel spring-pendulum combined SMA-STMD system, which utilises the mechanical properties of SMAs that change with temperature to achieve semi-active control. Finite element method simulations demonstrate that the proposed SMA-STMD system can effectively reduce structural seismic vibrations in CLT structure. By adjusting the SMA temperature, the SMA-STMD system can effectively address the issue of TMD system off-tuning caused by changes in the CLT structural properties. Overall, the proposed SMA-STMD system offers a promising solution for seismic control in CLT structures and has the potential to promote the development of CLT structures.

1. Introduction

In recent years, with the emergence of new engineered wood products, the height of timber structures has been increasing, making timber structure a popular trend in the global construction industry. Cross laminated timber (CLT) is a type of high-strength solid wood panel created by bonding wood boards in alternating directions. It can be used as shear wall in the construction of modern timber structures, as well as in steel-timber and concrete-timber hybrid structures. In 2012, Australia built a 9-story CLT building called Forte, measuring 32.2 m. Compared to reinforced concrete structures, it reduced carbon dioxide emissions by 1,451 tons [1]. In 2017, the University of British Columbia in Canada built an 18-story CLT student apartment measuring 54 m. By using prefabricated components in construction, it reduced building waste by two-thirds and decreased carbon dioxide emissions by 2,432 tons compared to reinforced concrete structures [2]. Therefore, building more modern timber structures can be a significant way to reduce the carbon emissions and achieve the net zero target and the Sustainable Development Goals of United Nations. In the future, more and more tall timber structures are being designed and built, with increasing heights and number of stories.

Compared to traditional building materials like concrete and steel, CLT structures have a good strength-to-weight ratio and high ductility. However, due to lower stiffness of timber, multi-storey CLT structures could be susceptible to have larger responses under earthquake loads [3,4]. Therefore, further development of multi-storey CLT structures requires a reduction in their seismic response. Researchers worldwide have gradually completed CLT connection tests [5,6], CLT shear wall tests [7,8], CLT structural pseudo-dynamic tests [9,10], and CLT structural shaking table tests [11]. Austria and Japan have conducted shaking table tests on full-scale 3-storey and 5-storey CLT structures [12,13]. In 2013, the CNR-IVALSA research institute in Italy conducted shaking table tests on a full-scale 7-storey CLT structure at NIED Miki in Japan as part of the SOFIE project [14]. The research results have shown that CLT materials have excellent ductility, and the seismic response of CLT structures is better than expected. However, shaking table tests have found that the peak acceleration of multi-storey CLT structures is high. In a very short time period, the top storey acceleration of the full-scale 7-

* Corresponding author.
E-mail address: haoyu.huang@newcastle.ac.uk (H. Huang).

https://doi.org/10.1016/j.istruc.2023.105093
Received 5 May 2023; Received in revised form 25 July 2023; Accepted 17 August 2023
Available online 23 August 2023

layer CLT structure reached 3.8 g, which could cause serious damage to non-structural components and cause some injuries to occupants [14,15]. The SOFIE project [14] concluded that reducing top storey acceleration response is a key research direction for future seismic research on multi-storey CLT structures and suggested that dampers could be used for seismic control in future studies.

The tuned mass damper (TMD) system is a convenient and economical vibration control measure that has gained attention and research across various fields since its concept was introduced by Den Hartog in 1956 [16]. Studies have found that TMD systems have significant vibration reduction effects in structures and have rapidly developed [17]. Poh'sié et al. [15,18] have innovatively applied the TMD system to a full-scale, multi-storey CLT structure to resist seismic action and found that under optimal tuning, and the TMD system can effectively reduce the seismic response of multi-storey CLT structures. However, there are limitations to the application of TMD systems in multi-storey CLT structures: (1) During the structural design process, calculating the natural frequency of the structure accurately is challenging because timber is a natural material [19], and the installation of TMD can cause a certain degree of frequency drift [16], which can significantly affect the control effect of TMD; (2) CLT structures are lightweight [3]. The mass of the structure can easily change due to human movement and facility relocation, which can affect the natural frequency of the CLT structure (previous studies by the authors have reported that the natural frequency of timber structural systems can easily change due to changes in mass [20,21]); (3) The stiffness of CLT structures can easily change due to factors such as material aging, moisture content, and further reinforcement during use [22]. Changes in stiffness and mass can have a significant impact on the seismic reduction effect of TMD. In general, the natural frequencies of the TMD system and the controlled structure must be the same or similar to achieve resonance effects. Otherwise, the TMD system will face serious offtuning problems, leading to greater structural vibration. Therefore, how to design TMD systems to control the seismic performance of multi-storey CLT structures is a research problem that needs to be addressed.

The application of semi-active tuned mass dampers (STMD) can solve the problem of offtuning in TMD systems. STMDs can adjust their own dynamic characteristics, expand their frequency domain control range, and effectively adapt to the conditions where the dynamic characteristics of the controlled structure are changed. STMDs have been researched and verified to have better vibration reduction performance than passive TMDs [23]. Recently, innovative materials have been investigated for structural engineering applications, such as functionally graded porous, composite materials and shape memory alloy (SMA) [24–27]. Their performances have been investigated subjected to thermal and mechanical loading fields. This study aims to explore the application of a new smart material - SMA - in STMDs to form an SMA-STMD system, as the dynamic characteristics of the STMD can be adjusted by changing the temperature of SMA [23,28]. Compared with traditional STMDs [29,30], the advantages of SMA-STMDs mainly focus on three aspects: (1) SMAs have superelastic performance, which means that even after yielding, the material has the ability to recover to the stress–strain origin, which can greatly reduce the residual deformation of the damper material [31–33] and enhance the robustness of STMDs; (2) SMA characteristics can be controlled by temperature, which can solve the problem of offtuning in the structure. Previous research has also found that SMA temperature control has a fast response speed [34]; (3) SMA can provide semi-active control relying on its own material properties, with simple mechanical structures that will not cause significant loads or space burdens on the structure.

Our pilot studies have explored whether the SMA-STMD can be used to control vibration by adjusting the temperature of the SMA in order to mitigate the structural vibration. Through vibration control experiments on a cantilever steel beam structure, the feasibility of the concept of using SMA temperature control for STMD vibration control was verified [28]. Subsequently, a scaled two-storey steel frame structure has been tested, and the results showed that the SMA-STMD can effectively address the problem of offtuning caused by changes in the controlled structure's mass [35]. However, the research on application of SMA-STMD to a full-scale multi-storey CLT structure to address the potential offtuning problems is still scarce, and previous research only focused on the feasibility research on scaled and laboratory-size models. To overcome this limitation, this paper will adopt the full-scale SMA-STMD to improve the seismic performance of multi-storey CLT structures. This paper aims to reduce the excessive acceleration response in CLT structures under seismic action using SMA-STMD and enhance the robustness of tuning by avoiding the offtuning during use.

This paper can be outlined as follows: 1) Controller, 2) Controlled Object, and 3) Application of the Controller to the Object. Specifically, 1) Controller: Section 2 focuses on the design and testing of the SMA-STMD. 2) Controlled Object: Section 3.1 is dedicated to the modelling of the CLT structure. 3) Application of the Controller to the Object is explored in Sections 3.2, 3.3, and 3.4, which delve into the application of the SMA-STMD to the CLT structure. Section 4 is the Discussion.

2. Test of SMA-STMD

2.1. SMA material

Among various families of SMA, Ni-Ti SMA has matured in its development, and possesses excellent material properties with good temperature sensitivity [28] and long fatigue life [36], making it suitable for semi-active control in STMD. The experimental results [36] affirm that both SMAs with different phase transformation temperatures exhibit stable mechanical behaviours and possess a long fatigue life. Additionally, Ni-Ti SMA has smaller grain size, which reduces the risk of grain boundary fracture. Therefore, all SMAs used in this study is Ni-Ti (Ni56% and Ti44%) SMA, and they are provided by Xi'an SaiTe Metal Materials Development Co., Ltd. Differential Scanning Calorimetry (DSC) tests were conducted on a 13.6 mg sample of the Ni-Ti SMA, with temperature settings ranging from −40℃ to 100℃. The phase transformation temperatures of SMA were found to be M_f = -11.1℃, M_s = -9.3℃, As = -2.2℃, and A_f = 25.7℃. The temperatures M_s and M_f refer to the start and finish temperatures of the Martensite transformation, which is a phase transformation that occurs in SMA when it undergoes a cooling process. On the other hand, A_s and A_f denote the start and finish temperatures of the Austenite transformation. Austenite is a phase at elevated temperatures. Through a monotonic tensile test on a Ni-Ti SMA dog bone bar with a diameter of 10 mm and an effective length of 30 mm at room temperature (20℃), the elastic modulus and strength were determined to be 35.4 GPa and 822 MPa, respectively. Fig. 1 depicts the

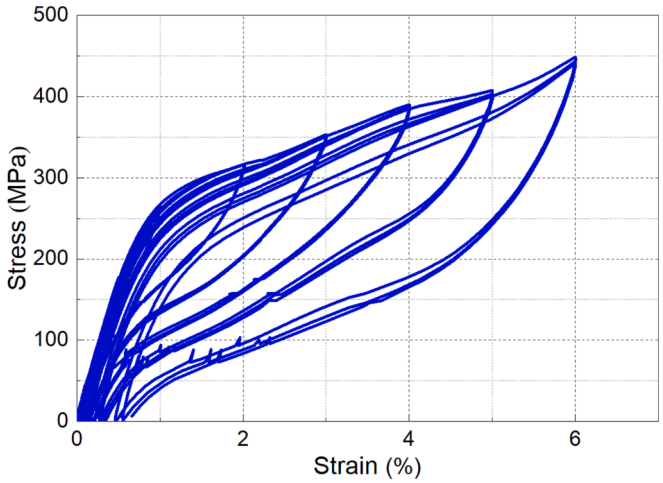

Fig. 1. Stress–strain relationship of Ni-Ti SMA bar.

stress–strain hysteresis of the Ni-Ti SMA bar under cyclic tensile loading using displacement control at room temperature, exhibiting typical superelastic behaviour.

2.2. Setting-up of the SMA-STMD

The SMA-STMD system designed in this study is a combination of pendulum-type TMD and spring-type TMD, and it is an improvement over the design presented in [23]. In [23], the mass block was suspended by the SMA bar, which caused the mass block to provide a pre-stress to the SMA bar. However, this approach is not feasible in a full-scale TMD where the block mass is heavy. For SMA-STMD in this study, steel cables have been used to support the weight of the steel block, while SMA bars are placed under the steel block and utilised to adjust the dynamic characteristics of the STMD. The mechanical model of application of the SMA-STMD to a structure is presented in Fig. 2. The function of SMA bars can be simplified into springs. The controlled structure is simplified as a single-degree-of-freedom system with mass m_1, stiffness k_1, and damping c_1. The external load applied to the controlled structure is denoted as F_1. The stiffness of the SMA-STMD system, k_2, is provided by four Ni-Ti SMA bars placed in parallel to provide bending stiffness. The mass of the steel block is denoted as m_2, with damping c_2, and l represents the distance between the mass centre of the steel mass block and the top of the steel frame. h is distance between the universal joint on the top of the SMA bars and the top of the steel frame.

The motion equations can be derived from the mechanical model shown in Fig. 2 using the principle of virtual work:

$$-\delta W_s = k_2\theta(t)h\delta(\theta(t)h) + k_1x_1(t)\delta x_1(t) = k_2h^2\theta(t)\delta\theta(t) + k_1x_1(t)\delta x_1(t) \tag{1}$$

$$-\delta W_D = c_2\dot{\theta}(t)h\delta(\theta(t)h) + c_1\dot{x}_1(t)\delta x_1(t) = c_2h^2\dot{\theta}(t)\delta(\theta(t)) + c_1\dot{x}_1\delta x_1(t) \tag{2}$$

$$\begin{aligned} -\delta W_I &= m_2\left(l\ddot{\theta}(t) + \ddot{x}_1(t)\right)\delta(l\theta(t) + x_1(t)) + m_1\ddot{x}_1(t)\delta x_1(t) \\ &= m_2l^2\ddot{\theta}(t)\delta\theta(t) + m_2l\ddot{x}_1(t)\delta\theta(t) + m_2l\ddot{\theta}(t)\delta x_1(t) + m_2\ddot{x}_1(t)\delta x_1(t) \\ &\quad + m_1\ddot{x}_1(t)\delta x_1(t) \end{aligned} \tag{3}$$

$$\delta W_p = -m_2g\theta(t)\delta(l\theta(t)) = -m_2gl\theta(t)\delta\theta(t) + F_1(t)\delta x_1(t) \tag{4}$$

Combine Equations (1), (2), (3) and (4):

$$m_1\ddot{x}_1(t) + c_1\dot{x}_1(t) + k_1x_1(t) + m_2l\ddot{\theta}(t) + m_2\ddot{x}_1(t) = F_1(t) \tag{5}$$

$$m_2l^2\ddot{\theta}(t) + c_2h^2\dot{\theta}(t) + \left(k_2h^2 + m_2gl\right)\theta(t) + m_2l\ddot{x}_1(t) = 0 \tag{6}$$

By using Equations (5) and (6), the motion equation of the SMA-STMD can be derived as Equation (7):

$$\begin{bmatrix} m_1+m_2 & m_2l \\ m_2l & m_2l^2 \end{bmatrix}\begin{bmatrix} \ddot{x}_1(t) \\ \ddot{\theta}(t) \end{bmatrix} + \begin{bmatrix} c_1 & 0 \\ 0 & c_2h^2 \end{bmatrix}\begin{bmatrix} \dot{x}_1(t) \\ \dot{\theta}(t) \end{bmatrix} + \begin{bmatrix} k_1 & 0 \\ 0 & m_2gl+k_2h^2 \end{bmatrix}\begin{bmatrix} x_1(t) \\ \theta(t) \end{bmatrix} = \begin{bmatrix} F_1(t) \\ 0 \end{bmatrix} \tag{7}$$

The natural frequency of the SMA-STMD can be calculated in Equation (8):

$$f_2 = \frac{1}{2\pi}\sqrt{\frac{g}{l} + \frac{k_2}{m_2}\left(\frac{h}{l}\right)^2} \tag{8}$$

where g denotes the acceleration of gravity. The derived equations play a crucial role in demonstrating the design considerations and parameters of the SMA-STMD. These equations form the foundation for the subsequent modelling of the SMA-STMD.

The controlled structure is chosen to be the 7-storey CLT structure in the SOFIE project [14]. The controlled structure has the natural frequency of 2.34 Hz in x direction and 3.34 Hz in y direction. To design a TMD for that, the optimal frequency ratio under seismic loading is set to be 0.96 for a mass ratio of 0.01 according to [15]. Thus, the natural frequencies of the TMD system in the x and y directions aim to be around 2.25 Hz and 3.21 Hz, respectively. Based on Equation (8), the dimensions of the SMA-STMD system can be determined and the constructed laboratory model is illustrated in Figs. 3 and 4. It consists of six main components: a steel frame, four steel cables, a steel mass block, four universal joints, four Ni-Ti SMA bars, and a steel bottom plate. The mass block is a steel cube with a weight of 0.9648 t, suspended by four steel cables to support its entire weight. As shown in Fig. 4 (a) and (b), the four steel cables are hinged to the top of a steel frame with dimensions of 0.9 m × 0.9 m × 0.9 m. Four SMA bars are placed under the steel cube, as seen in Fig. 3 (a) and Fig. 4 (c). The parameters of the SMA-STMD were designed based on Equation (8). The key dimensions are: steel cube side length $a = 503$ mm, steel cable length $b = 150$ mm, length between steel cube centre and oscillation centre $l = 477$ mm, length between hinge centre and oscillation centre $h = 789$ mm and steel frame height $H = 900$ mm. The top of the SMA bars is connected to the steel cube using universal joints which are hinges, while the foot of the SMA rods is fixed on the steel bottom plate. This boundary condition ensures that the SMA bars bend instead of being sheared when the steel mass block sways. The cross-section of the upper and lower gripping sections of the SMA bars is round and larger than that in the effective zone, as presented in Fig. 3 (b), to facilitate the bending occurring in the effective zone. In terms of SMA bars, each gripping section plus the transition zone is 20 mm long, and the effective zone is 30 mm long. To enable the TMD system to function in both the x and y directions, the effective cross-section of the SMA rod is designed as a rectangle with dimensions of 15 mm (x direction) × 25 mm (y direction), providing different bending stiffness in the x and y directions for the TMD system. After a free vibration testing, the natural frequencies of the SMA-STMD are 2.09 Hz in x direction and 3.32 Hz in y direction, respectively, which are similar with the target frequencies.

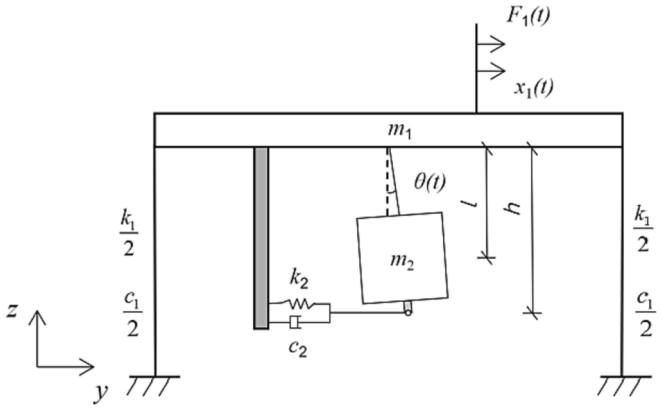

Fig. 2. Mechanical model of SMA-STMD applied to a controlled structure.

2.3. Methods

To control the SMA-STMD by changing the temperature of SMA, it is important to investigate the effect of temperature changes on the dynamic characteristics of the SMA-STMD system. Also, the effective frequency domain for semi-active control should be obtained.

The dynamic characteristics were determined by free vibration. This study chose x direction as a case study for control. An initial displacement of 50 mm was applied to the steel mass block in the x direction to enable free vibration. An accelerometer was installed on the steel mass block to obtain the acceleration time history, with a sampling frequency of 1000 Hz. The temperature of the SMA can be adjusted. The cooling

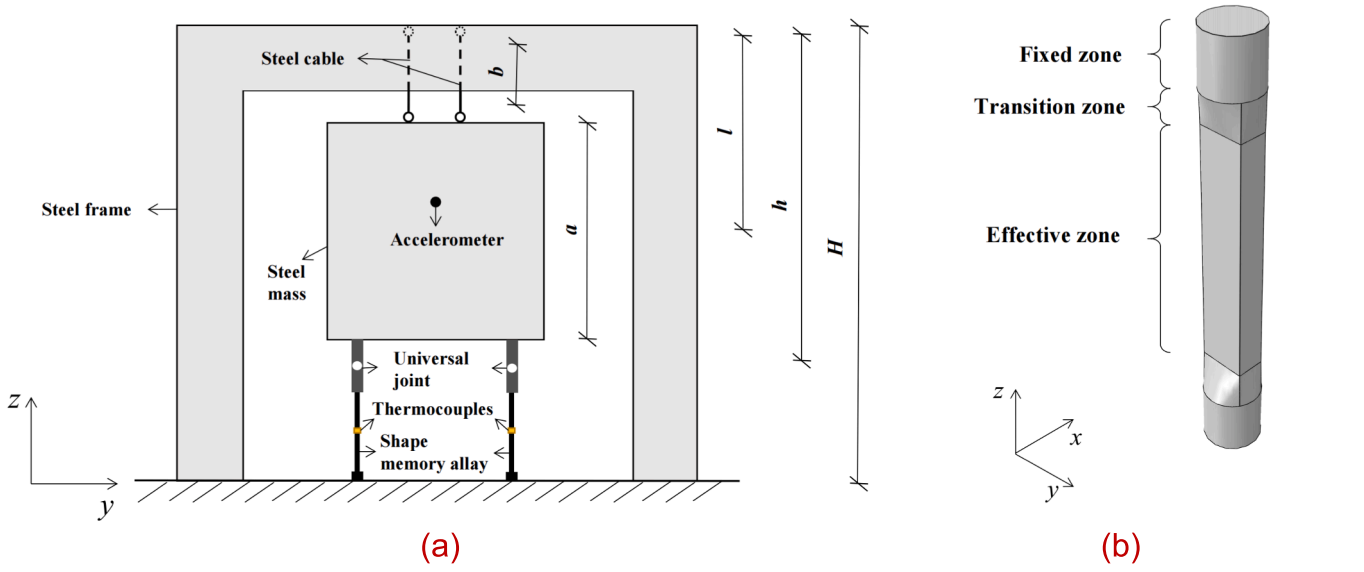

Fig. 3. (a) Schematic diagram of SMA-STMD; (b) SMA bar in the SMA-STMD.

was achieved by spraying 1,1,1,2-Tetrafluoroethane, and the heating was achieved by using electric blowers. Four thermocouples were attached to the outer surface of the middle section of the four SMA bars. After the temperature was raised or lowered, the temperature of the SMA bars was kept constant for 2 min before the free vibration test began. This step allowed the internal temperature of the material to equilibrate and accounted for the heat transfer effects. By stabilising the temperature of the SMA, this process contributed to maintaining the accuracy and reliability of the experimental results.

The first step of the test was to measure the acceleration time history of the SMA-STMD system in the x-direction free vibration under room temperature (20℃) for 20 s. The second step was to control the working temperature of the SMA bars to vary from −40℃ to 80℃, with a temperature interval of 10℃, and measure the acceleration time history of the SMA-STMD system in the x-direction free vibration for 20 s in each temperature. The natural frequency and damping ratio of the SMA-STMD can be analysed by the Matrix Pencil method [37,38] using the measured acceleration timber history.

2.4. Results

The variations of the natural frequency and the damping ratio of the SMA-STMD are shown in Fig. 5, indicating that the natural frequency of the SMA-STMD system increased and the damping ratio decreased with the temperature rise. When the temperature increases from −40℃ to 80℃, the natural frequency increased from 1.88 Hz to 2.30 Hz (Fig. 5 (a)). The reason is that the temperature can change the elastic modulus of the SMA, which has been proved in the previous research [23].

From Fig. 5 (b), the damping ratio decreased from 12.86% to 2.69% from −40℃ to 80℃. The Ni-Ti SMA used in the test had phase transition temperatures of M_f = -11.1℃, M_s = -9.3℃, As = -2.2℃, and A_f = 25.7℃. From −2.2℃ to 25.7℃, the SMA underwent a phase transformation from martensite to austenite, and at this stage, it was in a mixed state of martensite and austenite. From 25.7℃, it was the disappearance of martensite, and the SMA exhibited its superelastic properties. When the temperature was reduced below −11.1℃, SMA behaved in shape memory effect (SME), and it had a performance with larger energy dissipation.

In Fig. 5, the influence of temperature on natural frequency is modelled as a quadratic function while the influence of temperature on damping ratio is modelled as a linear function. The reason for this behaviour can be attributed to the phase transformation property of the SMA. According to the study conducted by Shaw and Kyriakides [39], the SMA undergoes a phase transformation into Martensite at temperatures at below 0℃, resulting in a low and constant loading transformation stress. In the Martensite phase, it can be observed that the transformation stress of the SMA becomes low and its stiffness remains relatively constant [39]. Consequently, the relationship between stiffness and temperature should follow a quadratic function. The paper [39] also observed that there was a linearly declined unloading transformation stress with the lower temperature, and the hysteretic loop is becoming larger. As a result, a linear function is employed to represent the damping ratio with the temperature.

Based on the analysis above, by curve fitting, the relationship between the natural frequency and the SMA temperature as well as the relationship between the damping ratio and the SMA temperature can be depicted by equations. As a result, the dynamic characteristics of SMA-STMDs, in terms of natural frequency and damping ratio, can be effectively adjusted by varying the temperature. This temperature-sensitive behaviour of SMA offers a promising way to improve the performance of structural vibration control systems.

2.5. Discussions

In this study, four SMA bars were used. In practical applications, more SMA bars can be placed in parallel to widen the frequency and damping ratio range. It is also possible to use SMAs with different phase transformation temperatures to achieve various temperature sensitivities. Since the size of the SMA bars may vary in practical use, the transfer of heat and the effect of temperature on stiffness may differ. In the future, more advanced and effective heating or cooling measures can be adopted, such as using direct current voltage control for Joule heating of the SMA bars.

3. Application of SMA-STMD to the CLT structure for seismic control

The Section 3 revolves around assessing the effectiveness of the SMA-STMD on the CLT structure. To achieve this, the paper relies on FEM analysis, Section 3.1 models the CLT structure and Section 3.2 models the installation of the SMA-STMD. The testing is detailed in Sections 3.3 and 3.4. Section 3.3 serves as the methodology, and Section 3.4 then presents the results of this analysis.

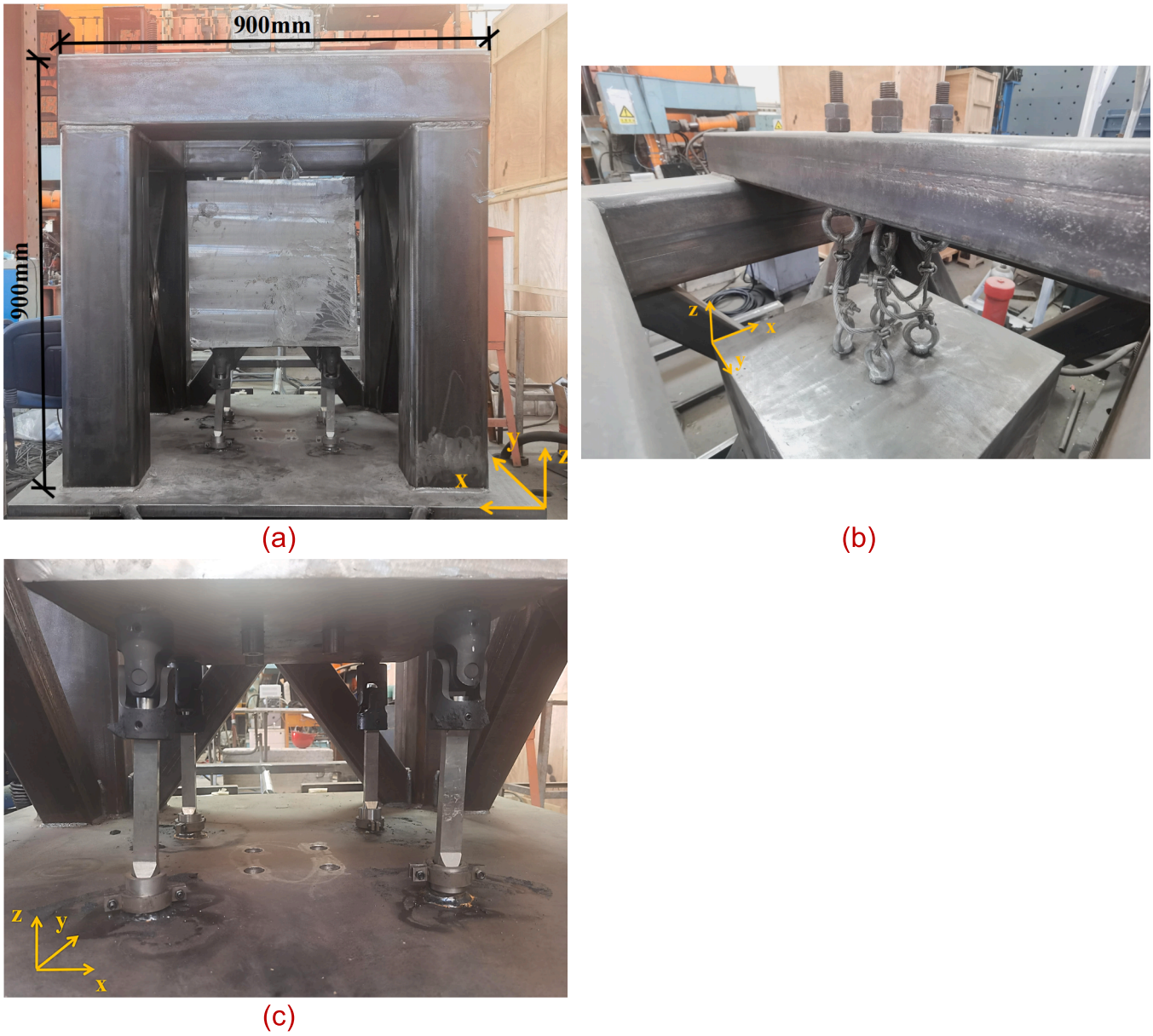

Fig. 4. Construction diagram of (a) the SMA-STMD; (b) the steel cables; (c) the SMA bars.

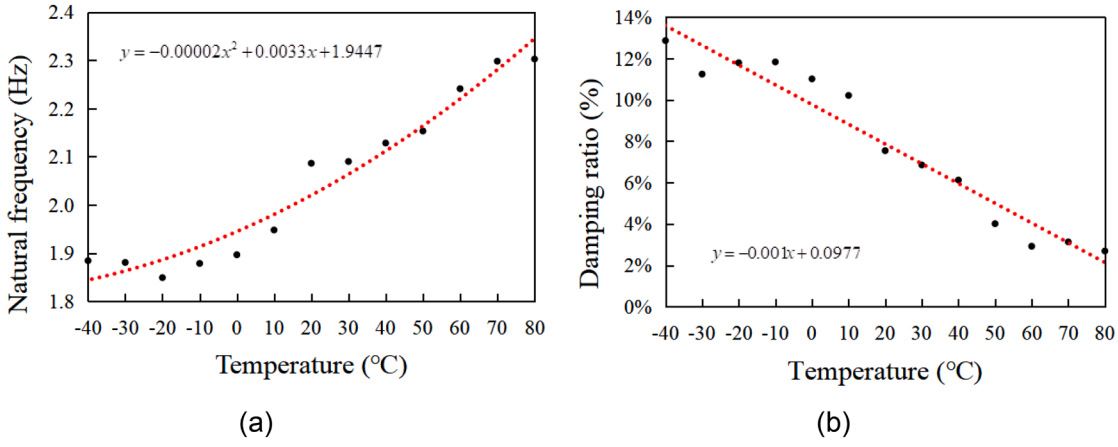

Fig. 5. Natural frequency (a) and damping ratio (b) change of the SMA-STMD with temperature change.

3.1. The CLT structure

This study aims to use finite element method (FEM) to investigate the vibration control performance of the SMA-STMD on the CLT structure. The controlled structure chosen in this study is the seven-storey CLT structure in the SOFIE project [14], as shown in Fig. 6, which was simulated using FEM software ABAQUS. Fig. 7 shows the plan and south elevation view of the CLT structure, with overall dimensions of 13.44 m in the x-direction and 7.68 m in the y-direction, and a structural height of 23.20 m. The thickness of CLT panels decreasing along the height: 142 mm for the first and second floors, 125 mm for the third and fourth floors, and 85 mm for the roof and other parts. The details in terms of mass of the CLT structure in the SOFIE experiment is also shown in [14], with a total weight of 278 t for the CLT structure simulated in this study using finite element analysis. Other details of the CLT structure are presented in [14].

Currently, there are three main methods for FEM modelling of CLT structures, which are the combination of elastic shell elements and nonlinear spring elements, the combination of elastic shell elements and linear spring elements, and a simplified method using nonlinear spring elements to simulate walls. In this study, the methods of elastic shell elements and elastic spring elements were used which referred to [15]. Fragiacomo et al. [40] have conducted a case study of the elastic seismic analysis of a multi-storey crosslam building under seismic actions. The results found that the elastic modelling led to an acceptable approximation of the wooden panel behaviour. Also, there was absence of nonlinear damage in the structural elements after the shaking table tests [14]. The absence of damage in the structural elements observed after the shaking-table tests allows for the use of an elastic model. Relative FEM modelling methods can be found in [15] in details. The S4R elastic shell elements with isotropic properties were used to simulate CLT floor slabs and wall panels. The elastic modulus of elasticity was calculated using the Blass-Fellmoser method [41], which averages the stiffness of the CLT panels in the vertical and horizontal directions, respectively, at 370 MPa and 11000 MPa. The elastic modulus of the five-layer CLT panels is estimated to be 5685 MPa [15]. There are three types of metal connectors between the CLT panels in the SOFIE experiment, namely, angle brackets, hold-downs, and screws. In the FEM model, each shell element is connected to another through elastic spring elements, simulating the connectors between CLT timber. The stiffness of each spring element is based on the values provided by [15]. The damping ratio of the structure is set to 2% using Rayleigh damping.

Fig. 8 shows the FEM model and mesh partition of the CLT structure. The natural frequencies of the FEM model of the CLT structure in the x and y directions are 2.18 Hz and 3.62 Hz, respectively. During the SOFIE full-scale test [14], the natural frequencies of the CLT structure in the x and y directions were 2.34 Hz and 3.32 Hz, respectively, with an error of less than 10% compared to the FEM modelling results. This level of error is acceptable given the uncertainties in the finite element simulation. However, a more complex nonlinear model could yield more precise results. When subjected to the JMA Kobe earthquake at the bottom of the CLT structure, the peak accelerations in the x and y directions are 3.9 g and 1.6 g, respectively. During the SOFIE test, the CLT structure experienced peak accelerations of 3.8 g in the x direction and 2.4 g in the y direction under the JMA Kobe earthquake, with an error within an acceptable range.

Fig. 6. The 7-storey CLT structure in SOFIE project [14].

3.2. Application of the SMA-STMD

A common mass ratio of 1–5% between TMD and the main structure is recommended because a ratio that is too low would have little effect, while a ratio that is too high would place a heavy loading burden on the floor slab. However, since the CLT floor has a lower stiffness compared to concrete or steel floors, a mass ratio of 1% was chosen for this study. To achieve this ratio, three SMA-STMDs were used and placed on the top floor of the CLT structure. Since the mass of each SMA-STMD is 0.964 t, applying three of them results in a mass ratio of 1.06%.

The FEM model of the SMA-STMD is presented in Fig. 10. To construct the steel frame, the B31 beam element was utilised to simulate the steel cable, universal joint sleeve, hinge block, cross hinge, SMA bars, and mass block. The bottom plate was modelled using the C3D8 solid element. All dimensions of the model parts were consistent with those of the full-scale SMA-STMD laboratory model in Section 2. The stress state of both the universal joint and SMA bar in the SMA-TMD system is of utmost importance. To accurately simulate the SMA-TMD system using FEM, the mesh division for these components is intentionally dense. Additionally, mesh refinement techniques were employed in areas with stress concentration, such as the connections between various parts. To achieve an optimal mesh, adaptive mesh refinement was utilised, and manual adjustments were made through face partitioning. Moreover, considering the irregular shapes of the universal joint, SMA bar components, and mass blocks, the C3D10M mesh generation mode was applied. The finer mesh size is 5 mm. The bottom plate, on the other hand, was meshed using the C3D8R mesh generation mode.

All materials used in FEM are identical to those in Section 2. To simplify the modelling, all the materials were modelled to be elastic. The energy dissipation property was modelled by setting the Rayleigh damping for the entire SMA-STMD system. The steel frame, universal joint, base plate, and steel cables were modelled using steel material, with their elastic modulus set to 2.06×10^5 N/mm^2 and Poisson's ratio set to 0.3. The SMA bar was modelled explicitly as shown in Fig. 11 (a), and the elastic modulus and dimensions of SMA were the same as the value in Section 2.

Fig. 11 (b) shows the FEM simulation of the universal joint of the top

Fig. 7. (a) Plan views of the CLT structure; (b) South elevation view of the CLT structure [14].

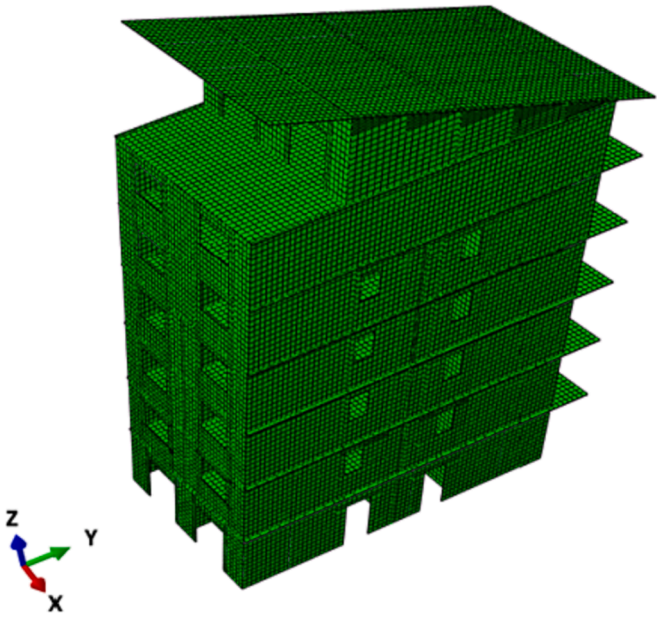

Fig. 8. FEM model of the CLT structure in Abaqus.

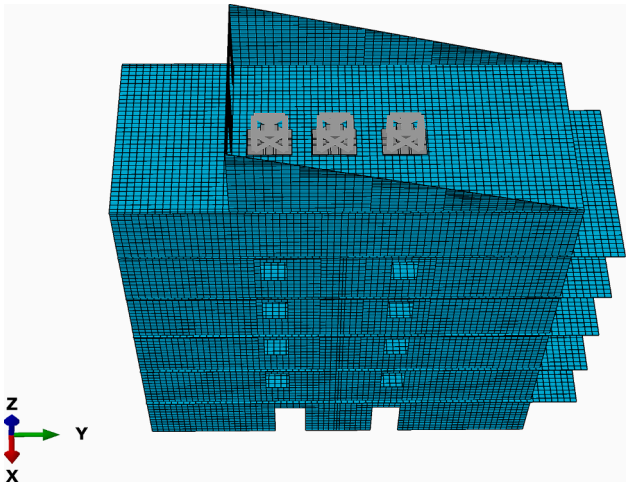

Fig. 9. Installation of the SMA-STMDs on the CLT structure.

of the SMA bar, which consists of three parts: upper and lower sleeves, a central hinge block, and a cross slide block. Hard contact is used to simulate the contact surfaces between the cross hinge and the upper and lower sleeves, and between the hinge block and the sleeves. Smooth contact is set to simulate the characteristic of the universal joint being able to rotate freely.

The modal analysis results of the SMA-STMD system are shown in Fig. 12. The first and second mode shapes were found to be swinging in the x and y directions, with natural frequencies of 2.09 Hz and 3.33 Hz, respectively. The natural frequencies in both directions were close to those measured in laboratory tests (2.09 Hz and 3.32 Hz), indicating that the FEM modelling was effective. This provides a foundation for the subsequent FEM simulation of the SMA-STMD system applied to CLT structures.

Based on the free vibration tests of the SMA-STMD system in Section 2, the natural frequency and damping ratio of the system are found to vary with changes in temperature of the SMA bar. In Abaqus, it is possible to simulate this effect by adjusting the elastic modulus of the SMA to reflect the change in natural frequency and modifying the Rayleigh damping to account for the change in damping ratio caused by temperature.

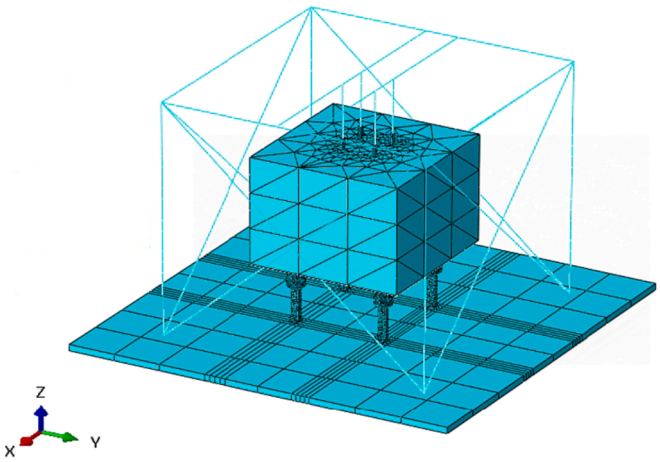

Fig. 10. FEM model of the SMA-STMD system.

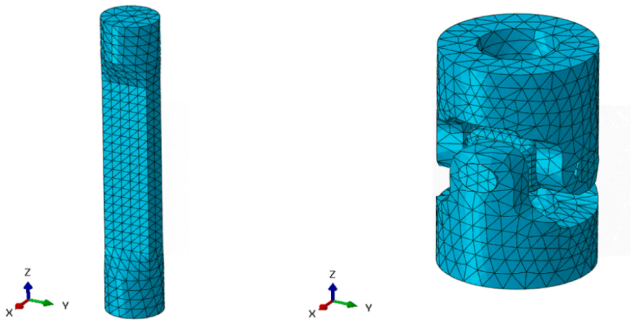

Fig. 11. (a) FEM model of SMA bar; (b) FEM model of the universal joint.

3.3. Testing plan

In this section, the dynamic performance of the CLT structure with and without three SMA-STMDs was investigated under seismic loading. All the investigations were based on Abaqus modelling, and the CLT model and the SMA-STMD model built in Sections 3.1 and 3.2 were employed. The El Centro earthquake can cause strong vibrations lasting between 1.5 and 5.5 s, with a dominant frequency range of 0.39–6.39 Hz. The first and second natural frequencies of the CLT structure were within this frequency range. In structural engineering applications, seismic forces are random and have a broad frequency range. Therefore, this is the reason why the non-scaled El Centro earthquake was selected to validate the effectiveness of the SMA-STMD measures on the CLT structure. The earthquake wave for input was El Centro seismic wave (Imperial Valley) in NS direction with PGA of 0.35 g, and the magnitude is 7.1.

The earthquake was performed in x direction (Fig. 9) as a case study, which is in line with the deformation direction of the structural first mode shape. Although it is important to acknowledge the need for comprehensive coverage, analysing the y direction would be redundant as it would essentially involve re-examining the same control theory. Therefore, only x direction is tested in this study. The seismic performance of the CLT structure was evaluated through various tests, as depicted in Fig. 13 and summarised in Table 1. Test 1 examined the structural behaviour without TMD, while Test 2 involved the use of a tuned SMA-STMD. Tests 3 and 4 were conducted with offtuned SMA-STMD. The offtuning scenarios were induced by modifying the CLT structural properties. In Test 3, the natural frequency decrease was achieved by reducing the elastic modulus of the CLT, which could occur in real-life scenarios due to material deterioration caused by high moisture content or aging. In Test 4, the natural frequency increase was modelled by decreasing the structural mass, which could result from human or equipment relocation in the building. Tests 2, 3 and 4 specifically investigate the performance of a passive TMD (traditional TMD) under consideration. In these tests, the semi-active control function was turned off and it became a passive TMD. Finally, Tests 5–8 explored the retuning by adjusting SMA temperature on the SMA-STMD accordingly. The details of the retuning are described in Sections 3.4.2 and 3.4.3.

3.4. Results

3.4.1. Effectiveness of SMA-STMD

Fig. 14 shows the application of SMA-STMD on the top of CLT structure under El Centro earthquake. Fig. 14 (a) presents the acceleration time history curves in the x-direction of the mass centre of the top floor in Tests 1 and 2. As shown in Table 1, the reduction in top-storey peak acceleration amplitudes is 28.00% from Test 1 to Test 2, while the reduction in RMS acceleration amplitudes is 39.24%. Fig. 14 (b) shows the peak acceleration per storey of the CLT structure in Tests 1 and 2, and it proves that the tuned SMA-STMD is effective to reduce the vibration in each storey and the effectiveness become more significant in higher storey. The results are aligned with the expectations.

In summary, Fig. 14 provides strong evidence that SMA-STMD is an effective solution for reducing the vibration response of CLT structures under earthquake loading. The results suggest that SMA-STMD can be a viable alternative for seismic protection of CLT structures.

3.4.2. Offtuning caused by deteriorating and its retuning

The results presented in Fig. 15 (a) and Table 1 reveal that the peak acceleration at the top of the CLT structure increased significantly from 1.471 g in the tuned state of Test 2 to 2.025 g in the offtuning condition of Test 3. This represents a 37.66% increase in peak acceleration and a 57.24% increase in RMS acceleration. 2.025 g is close to the peak acceleration of 2.043 g at the top of the CLT structure without the TMD

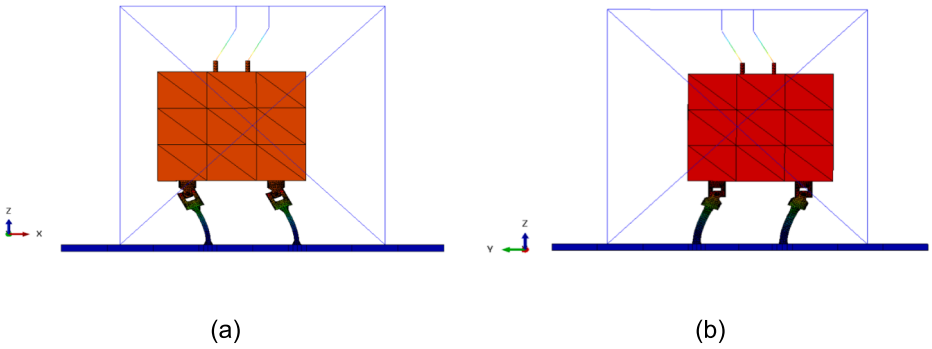

Fig. 12. Modal analysis of SMA-STMD system: (a) First mode shape in x direction; (b) Second mode shape in y direction.

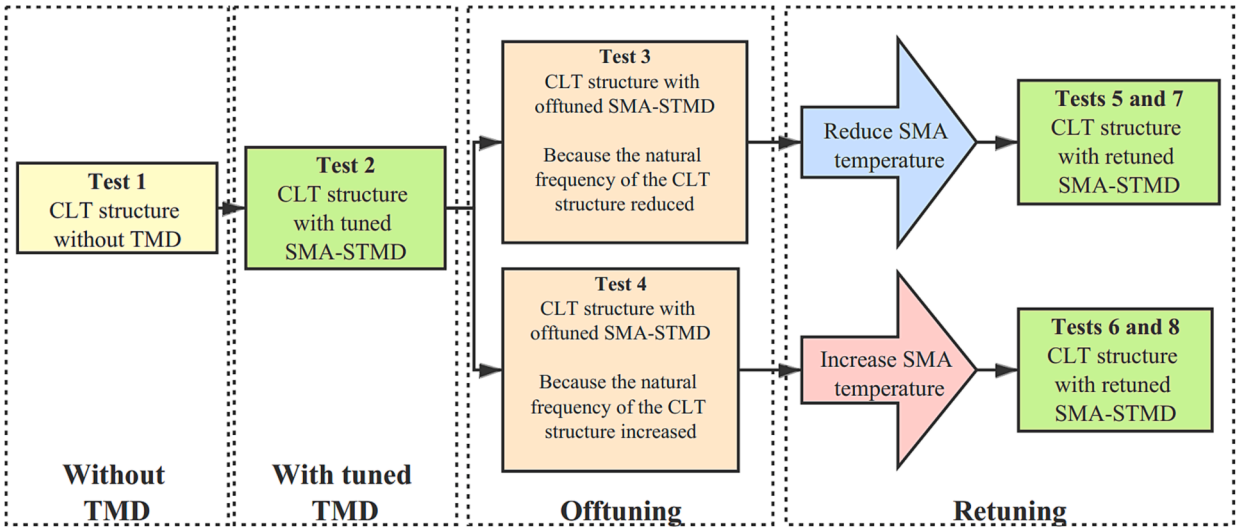

Fig. 13. Testing plan.

Table 1
SMA-STMD system applied to CLT structure tuning, offtuning and retuning.

	Without TMD (Test 1)	With SMA-STMD With tuned SMA-STMD (Test 2)	Natural frequency of CLT reduced (Test 3)	Cooling SMA to retune		Natural frequency of CLT increased (Test 4)	Heating SMA to retune	
				Test 5	Test 7		Test 6	Test 8
Mass of the CLT structure (t)	278	278	278	278	278	259	259	259
Elastic Modulus of CLT (MPa)	5685	5685	4000	4000	4000	5685	5685	5685
f_1(Hz)	2.18	2.18	1.99	1.99	1.99	2.25	2.25	2.25
Temperature of SMA (℃)	n/a	20	20	−40	−80	20	50	50
f_2(Hz)	n/a	2.09	2.09	1.90	1.81	2.09	2.16	2.16
ξ_2(%)	n/a	7.54	7.54	12.86	17.78	7.54	4.01	15.00
Peak acceleration (mm/s^2)	2.043	1.471	2.025	1.954	1.828	1.833	1.846	1.600
Reduction of the peak acceleration (%)	Reference	28.00	0.88	4.36	10.52	10.28	9.64	21.68
RMS acceleration (gal)	60.809	36.950	58.099	50.921	45.881	45.579	48.662	39.981
Reduction of the RMS acceleration (%)	Reference	39.24	4.45	16.30	24.55	25.05	19.98	34.25

f_1: Natural frequency of the CLT structure.
f_2: Natural frequency of the SMA-STMD.
ξ_2: Damping ratio of the SMA-STMD.

system. The acceleration per storey also showed a similar trend, indicating that the SMA-STMD system became ineffective in the offtuning condition. The results show a risk of using TMD system.

Two plans (Tests 5 and 7) were conducted to retune the SMA-STMD system as shown in Table 1. Test 5 cooled down the SMA to −40℃ and Test 7 cooled down the SMA to −80℃. Test 5 involved retuning the system to the optimal frequency ratio of 0.95, while Test 7 used a slightly lower frequency ratio of 0.91, but with a higher damping ratio of 17.78% achieved through cooling to have a more significant SME. The parameters of the retuned SMA-STMD in Tests 5 and 7 are presented in Table 1, based on the effect of temperature on the dynamic characteristics of the system as tested in Section 2.4.

From Table 1, the results indicate that Test 5 was effective in reducing the RMS acceleration by 12.35% and the peak acceleration by 3.51% compared to Test 3, confirming the success of the retuning process. In Test 7, the peak acceleration was reduced by 9.73% and the RMS acceleration by 21.03% compared to Test 3, demonstrating the effective retuning of the SMA-STMD system. In comparison, retuning in Test 7 is more effective. Importantly, the results suggest that taking advantage of the SME property of SMA in the retuning process can further enhance the energy dissipation. This was observed in Fig. 5, where cooling the SMA allowed for greater utilisation of SME. However, caution should be exercised to avoid excessive modification of the SMA stiffness.

3.4.3. *Offtuning caused by reducing structural weight and its retuning*

The second offtuning was caused by reducing the CLT structural mass from 278 t to 259 t. According to Table 1 and Fig. 16, by adjusting the structural mass in Test 4, the peak acceleration at the top of the CLT structure increased to 1.833 g and the RMS acceleration at top increased to 45.579 Gal compared to the tuned condition in Test 2. It can be found that the seismic performance with the offtuned SMA-STMD system became worse.

To address the problem, the retuning was performed to raise the frequency of the SMA-STMD system by increasing the temperature of SMA to 50℃ in Test 6. Based on the relationship concluded in Section 2.4, at this temperature, the frequency of the SMA-STMD system was 2.16 Hz, where the frequency ratio is 0.96. As shown in Table 1 and Fig. 16, when El Centro earthquake was applied to the CLT structure, the difference of the acceleration response between Test 4 and 6 is little. The reason is that the damping ratio of the SMA-STMD system decreased from 7.54% to 4.01% after heating SMA, which is less effective for seismic control.

Test 8 demonstrated that the natural frequency of the SMA-STMD can be adjusted by heating the SMA, while maintaining a sufficient

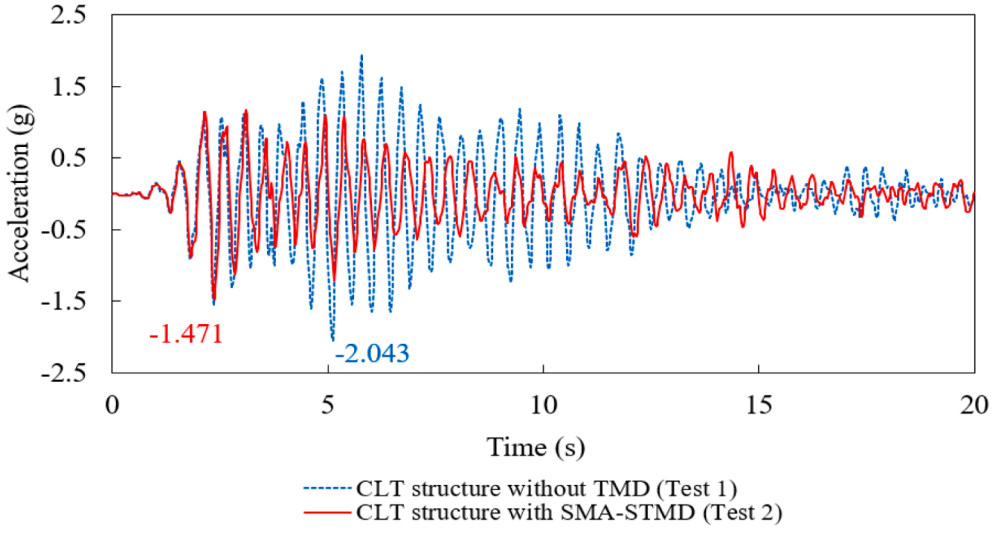

(a)

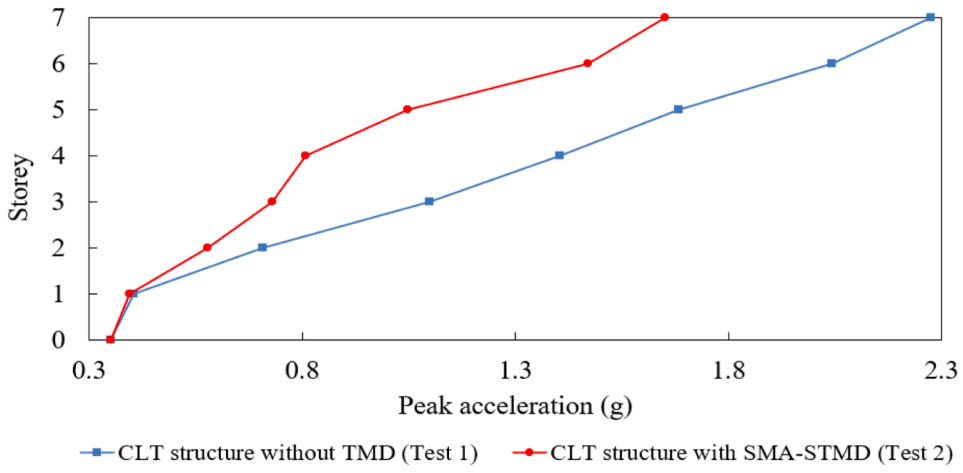

(b)

Fig. 14. (a) Acceleration time history of the CLT structure with SMA-STMD (Test 2) and without TMD (Test 1); (b) Peak acceleration per storey of the CLT structure with SMA-STMD (Test 2) and without TMD (Test 1).

damping ratio (15%) for TMD. This assumes that the SMA can maintain a high damping such as being prestressed or staying in SME without undergoing phase transformation. Fig. 16 and Table 1 show that under the retuning condition, the peak acceleration of the CLT structural top storey can be reduced by 12.71% compared to Test 4. Additionally, the RMS acceleration was reduced by 12.28%, indicating a satisfactory reduction effect. Thus, the SMA-STMD system with SMAs in higher damping of 15% can be effectively retuned. It can be found that using SMAs in higher damping provides an added advantage over passive damping systems that cannot be retuned. The potential for further improvements in damping through the use of SMAs is evident, and this study offers valuable insights into the efficacy of SMA-STMD systems in reducing structural vibrations.

The further direction for improving the SMA-STMD is to increase the damping capacity. Several solutions can be explored to address the limitation of lower damping in higher temperatures of SMA. One effective way of achieving higher damping in SMA is to apply a prestress to the SMA bars. This technique involves pre-bending the SMA bars, as shown in Fig. 17(a). The pre-bending process can use a hydraulic or mechanical press to bend the SMA bars to a certain degree. The amount of pre-bending required depends on the specific application and desired level of prestress. As shown in Fig. 17(b), prestressing the SMA bars causes a shift in the coordinate point to the top right, indicating a 'jump' over the elastic region. As a result, the SMA material can dissipate more energy and exhibit higher damping behaviour. To accurately achieve the targeted damping ratio, the implementation of temperature control can be utilised. The findings presented in Section 2.4 can serve as a valuable guide for adjusting the temperature accordingly. The temperature control can be achieved by electric heating and cooling and is aimed to be experimentally tested in the future.

In order to further enhance the damping properties of SMA-based systems, it is possible to select higher damping SMA materials. Additionally, the damping ratio of the SMA-STMD system can be increased by incorporating additional damping materials or components. The damping behaviour of Ni-Ti SMA is influenced by factors such as material composition, excitation frequency, and heat treatment method.

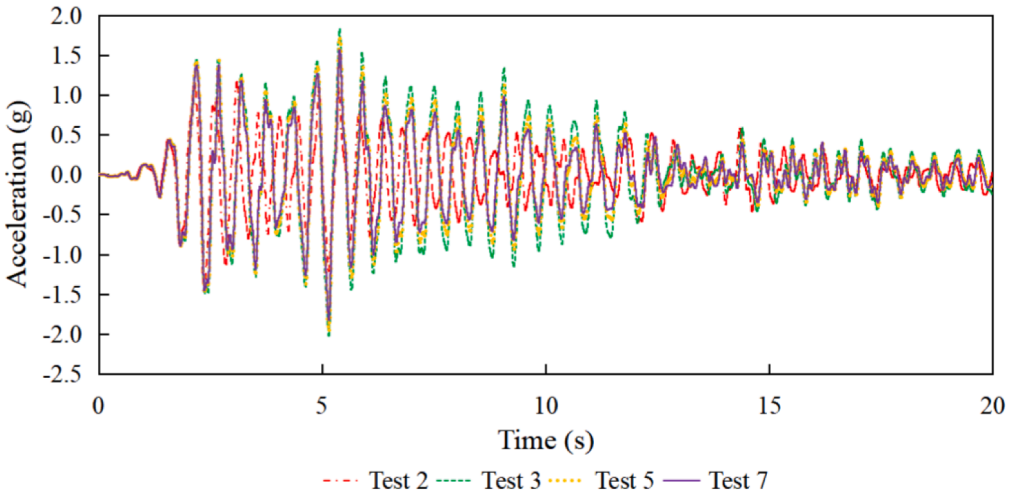

(a)

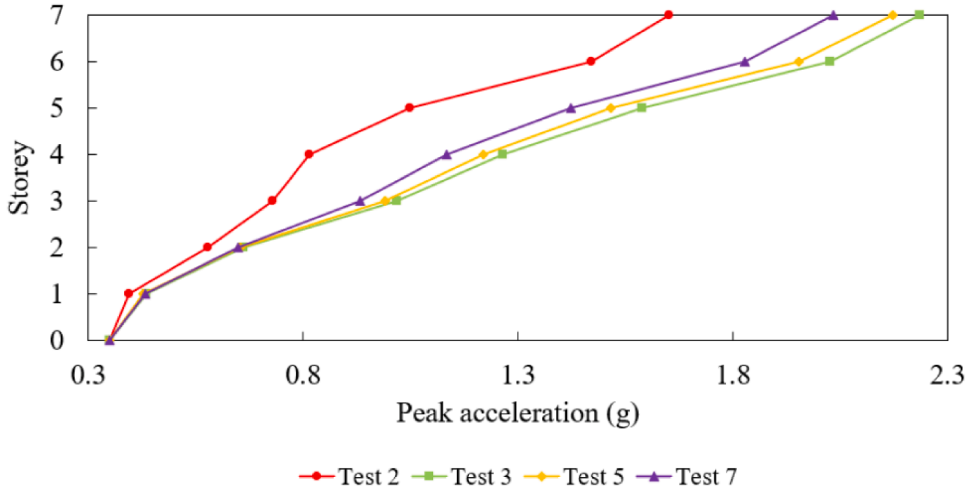

(b)

Fig. 15. (a) Acceleration time history curve at top storey and (b) peak acceleration per storey of the CLT structure during tuning (Test 2), offtuning (Test 3) and retuning (Tests 5 and 7).

Therefore, it would be beneficial to study and understand the factors that affect the damping of Ni-Ti SMA, and subsequently select SMA materials with higher damping properties, such as those with a broader range of Martensite. Increasing the phase transformation temperatures of the SMA can also have significant benefits for maintaining a high level of damping because it will be in its SME state. This can be achieved by altering the composition of the SMA material, which involves changing the ratios of various elements presenting in the alloy. For example, changing the nickel content or changing elements such as cobalt can change the transformation temperature, and an increase in annealing temperature also helps increasing the transformation temperature [42]. In addition to altering the composition of the SMA, another way to increase the phase transformation temperatures is through mechanical processing. Furthermore, shape memory polymer (SMP) composites can enhance the performance of SMA-STMDs. By embedding the SMA within an SMP matrix, the composite material can provide improved energy dissipation capabilities due to the damping properties of the polymer [43]. If there were accumulated residual strain in SME after cyclic deformation, heating would be used to remain the resilience. To enhance the damping of SMA-STMD, another option is to add more SMA bars in parallel to accumulate damping coefficients. This method helps to multiply damping coefficients and improve the overall performance of the system. Overall, the benefits of increasing damping in SMA-STMD are evident. The aforementioned solutions emphasise the potential for further improvement and development of SMA-STMD.

4. Discussion

To enhance the practicality of the SMA-STMD and make it more applicable for a wider range of applications, several measures can be taken to improve the dynamic characteristics of the system. One potential method is to enhance the heating and cooling equipment, which can expand the range of achievable temperatures and improve the versatility of the system. For example, incorporating more advanced heating and cooling systems, such as thermoelectric coolers or fluidic systems, can allow for more precise control of temperature gradients and enable the SMA-STMD to operate more effectively across a broader range of temperatures. Currently, there is a limited pool of references available for meaningful comparisons of the dynamic control technics on tall CLT structures. Moving forward, our research aims to incorporate

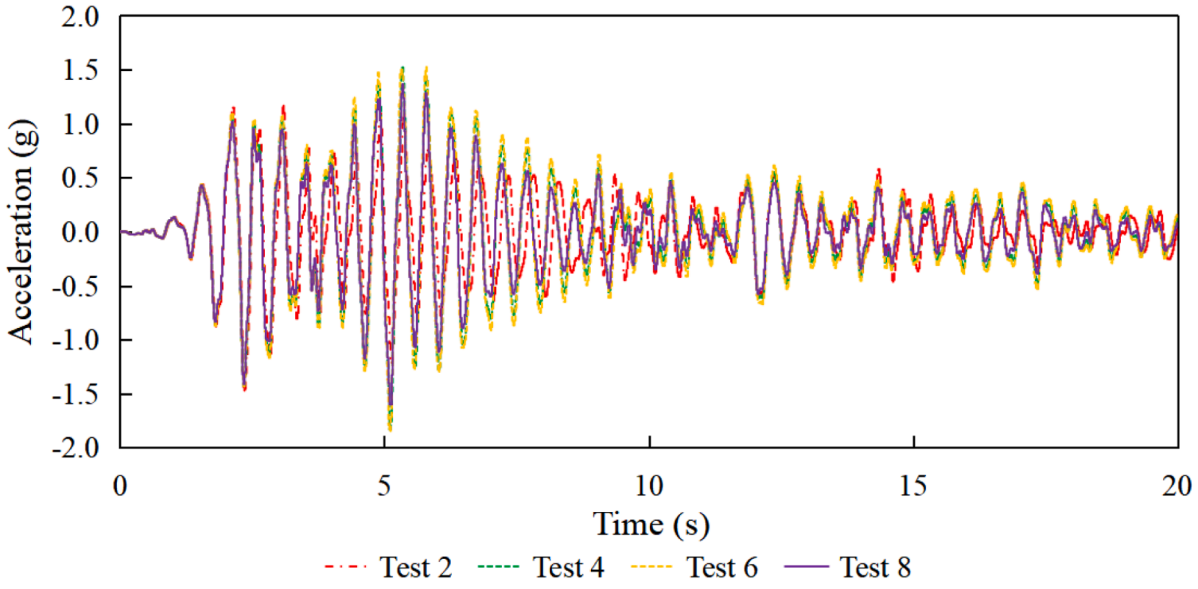

(a)

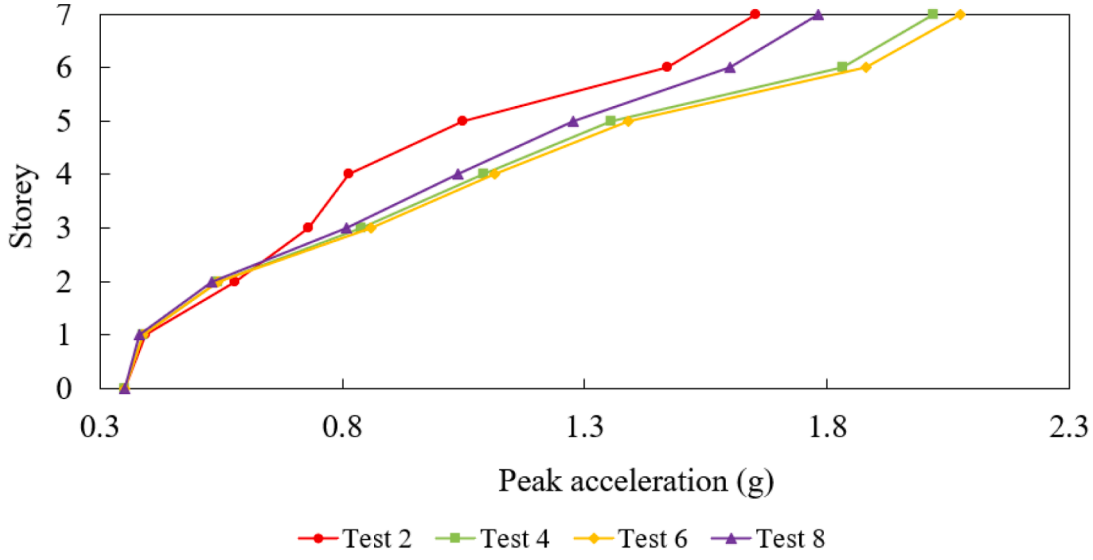

(b)

Fig. 16. (a) Acceleration time history curve at top storey and (b) peak acceleration per storey of the CLT structure during tuning (Test 2), offtuning (Test 4) and retuning (Tests 6 and 8).

a broader range of dynamic control methods in order to facilitate a comprehensive comparative analysis.

Another way to broaden the frequency band of the SMA-STMD is to increase the number of SMA bars used in the system. This can help to create various combinations to achieve different mechanical and thermomechanical properties. By doing these, the dynamic characteristics of the system can be more versatile. Additionally, by optimising the dimensions and configuration of the SMA bars and steel cable used in the SMA-STMD, it may be possible to further improve its performance and effectiveness. Other potential areas for development of the SMA-STMD include exploring alternative materials and manufacturing techniques for the SMA bars and steel cable. For instance, the use of advanced composites or alloys may allow for greater strength and stiffness while also reducing the weight and overall size of the system.

To enhance the practicality and applicability of SMA-STMD, the SMA-STMD can be designed to be adjusted to suit the practicality. For example, the sleeve of the bottom plate in the SMA-STMD system is designed to be detachable, allowing for easy replacement of SMA bars to adjust their size. Additionally, the length of the steel cable can be adjusted using bolts. In the future, the SMA-TMD system can be effectively combined with Structural Health Monitoring (SHM) technology to address the issue of maladjustment in specific frequency domains, which can have serious consequences for TMD systems. By implementing acceleration detection on controlled structures using SMA-TMD systems, it becomes possible to monitor structural behaviour. Signal processing techniques, coupled with artificial intelligence, machine learning, and related technologies, can be employed to rapidly calculate seismic and structural information. By adjusting the SMA temperature, the TMD

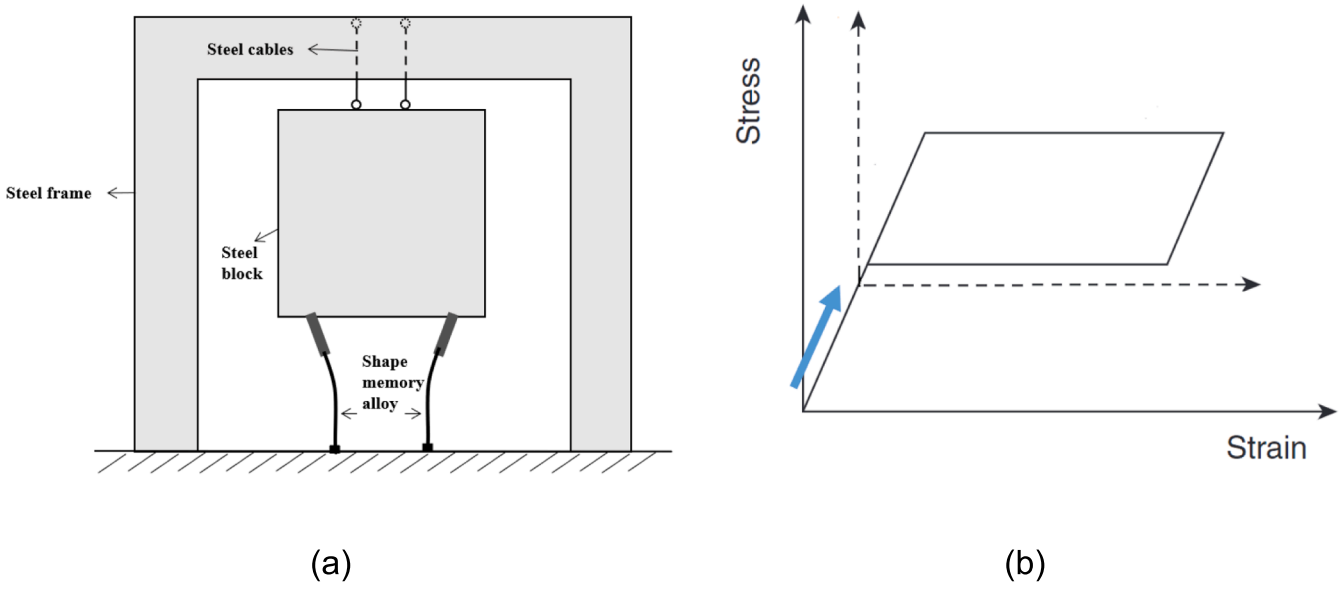

Fig. 17. (a) Prestressing SMA in the SMA-STMD; (b) The effect of prestressing on the stress–strain hysteresis of SMA.

system can be quickly retuned, enabling semi-active control of the controlled structure and effectively mitigating vibrations.

In practice, earthquakes are considered unpredictable events. Researchers have conducted several studies [44,45] that aim to establish optimal equations for TMD parameters under different types of seismic loadings. These studies provide valuable insights into achieving desirable performance of the TMD system. Building upon this existing research, this study aims to implement the semi-active control techniques to maintain these parameters of TMD at their optimal values. In other words, this study provides the control theory to maintain the TMD's parameters to be optimal for suiting different types of earthquake waves.

5. Conclusion

This study investigated the application of the SMA-STMD to the CLT structure for seismic vibration control. An innovative pendulum-spring combined SMA-TMD system was designed and tested through experimental tests, and the effect of temperature on its dynamic characteristics was obtained. Then, the SMA-STMD system was simulated using FEM. By conducting numerical modelling for a CLT structure, the effectiveness of the SMA-STMD control on the CLT structure was verified by simulating the tuning, offtuning, and retuning process.

The main conclusions are as follows:

The material properties of Ni-Ti SMA bar can be changed by varying temperature. The natural frequency of SMA-STMD decreased from 2.30 Hz to 1.88 Hz, and the damping ratio increased from 2.69% to 12.86% when the SMA temperature changed from 80℃ to −40℃.

The SMA-STMD system can effectively mitigate seismic vibration in CLT structures compared to the non-TMD condition. When subjected to the El Centro earthquake, the peak acceleration was reduced by 28.00%, and the RMS acceleration was reduced by 39.24%.

Changing the main structural properties can cause offtuning of the TMD, which can increase structural vibration. Retuning the SMA-STMD by cooling the SMA reduced the peak acceleration by 9.73% and the RMS acceleration by 21.03% compared to the offtuning condition.

By elevating the level of damping in the SMA, the effectiveness of the SMA-STMD in both cooling and heating can be enhanced, resulting in an improved retuning process.

This paper holds innovations. It proposes the theory of using SMA-STMD as a solution for controlling vibrations in CLT structures. The use of SMA-STMD is a novel approach that takes advantage of the mechanical properties of SMA, which change with temperature, to achieve semi-active control of structural vibrations. Additionally, the study offers a comprehensive design and examination of a full-scale SMA-STMD system. Both experimental and numerical methods are provided to assess the system's behaviour. Also, the study includes the specific FEM simulation techniques used to investigate the TMD system and its structural application. The proposed SMA-STMD system addresses the issue of excessive vibrations in CLT structures during earthquakes. It overcomes the limitations of traditional TMDs by utilising SMA and its ability to adjust properties based on temperature changes.

All in all, this technology holds immense potential for advancing the development of multi-storey CLT structures, further promoting sustainable construction practices. In the future, several solutions such as prestressing will be explored to increase the energy dissipation of SMA. More accurate and quicker temperature control approaches will be tested for the full-scale SMA-STMD system.

Declaration of Competing Interest

The authors declare that they have no known competing financial interests or personal relationships that could have appeared to influence the work reported in this paper.

Acknowledgement

The authors would like to thank the financial support from the Start-Up Funding at Newcastle University.

References

[1] Woodsolutions. *Forte Living*. 2023; Available from: https://www.woodsolutions.com.au/case-studies/forte-living.
[2] Nations, U., *Circularity concepts in wood construction* ed. C.o.F.a.t.F. Industry. 2022, Geneva: United Nations.
[3] Reynolds, T., et al., *Ambient vibration tests of a cross-laminated timber building.* Proceedings of the Institution of Civil Engineers-Construction Materials, 2015. **168** (3): p. 121-131.
[4] Feldmann, A., et al., *Dynamic properties of tall timber structures under ambient vibration*, in *World Conference on Timber Engineering*. 2016: World Conference on Timber Engineering.

[5] Gavric I, Fragiacomo M, Ceccotti A. Cyclic behaviour of typical metal connectors for cross-laminated (CLT) structures. Mater Struct 2015;48(6):1841–57.
[6] Huang HY, Chang WS. Seismic resilience timber connectionadoption of shape memory alloy tubes as dowels. Struct Control Health Monit 2017;24(10).
[7] Hristovski V, et al. Full-Scale Shaking-Table Tests of XLam Panel Systems and Numerical Verification: Specimen 1. J Struct Eng 2013;139(11):2010–8.
[8] Sun XF, et al. Performance evaluation of multi-storey cross-laminated timber structures under different earthquake hazard levels. J Wood Sci 2018;64(1):23–39.
[9] Lauriola, M.P. and C. Sandhaas. *Quasi-static and pseudo-dynamic tests on XLAM walls and buildings*. in *COST E29 International workshop on earthquake engineering on timber structures*. 2006. Coimbra.
[10] Popovski M, Gavric I. Performance of a 2-Story CLT House Subjected to Lateral Loads. J Struct Eng 2016;142(4).
[11] Ceccotti A. New Technologies for Construction of Medium-Rise Buildings in Seismic Regions: The XLAM Case. Struct Eng Int 2008;18(2).
[12] Flatscher, G. and G. Schickhofer, *Shaking-table test of a cross-laminated timber structure.* Proceedings of the Institution of Civil Engineers-Structures and Buildings, 2015. **168**(11): p. 878-888.
[13] Kawai N, et al. *Full scale shake table tests of five story and three story CLT building structures*, in *World Conference on Timber Engineering*. Vienna: Austria; 2016.
[14] Ceccotti A, et al. SOFIE project-3D shaking table test on a seven-storey full-scale cross-laminated timber building. Earthq Eng Struct Dyn 2013;42(13):2003–21.
[15] Poh'sie GH, et al. Application of a Translational Tuned Mass Damper Designed by Means of Genetic Algorithms on a Multistory Cross-Laminated Timber Building. J Struct Eng 2016;142(4).
[16] Den Hartog JP, Mechanical vibrations.. New York. London: McGraw-Hill; 1956.
[17] Rahimi F, Aghayari R, Samali B. Application of Tuned Mass Dampers for Structural Vibration Control: A State-of-the-art Review. Civil Engineering Journal-Tehran 2020;6(8):1622–51.
[18] Poh'sie GH, et al. Optimal design of tuned mass dampers for a multi-storey cross laminated timber building against seismic loads. Earthq Eng Struct Dyn 2016;45 (12):1977–95.
[19] Qian C, et al. Development of a Vibroacoustic Stochastic Finite Element Prediction Tool for a CLT Floor. Applied Sciences-Basel 2019;9(6).
[20] Huang H, Chang W-S. Application of pre-stressed SMA-based tuned mass damper to a timber floor system. Eng Struct 2018;167:143–50.
[21] Huang, H. and W.-S. Chang, *Reducing footfall-induced vibration in the timber floor system using a pre-stressed shape memory alloy-based tuned mass damper*, in *World Conference on Timber Engineering* 2018: Seoul.
[22] Porteous J, Kermani A. Structural timber design to Eurocode 5. 2nd ed. Chichester: Wiley-Blackwell; 2013.
[23] Huang HY, Mosalam KM, Chang WS. Adaptive tuned mass damper with shape memory alloy for seismic application. Eng Struct 2020;223.
[24] Zhang Q, et al. Stability of submarine bi-material pipeline-liner system with novel polyhedral composites subjected to thermal and mechanical loading fields. Mar Struct 2023;90:103424.
[25] Li Z, et al. Buckling performance of the encased functionally graded porous composite liner with polyhedral shapes reinforced by graphene platelets under external pressure. Thin-Walled Struct 2023;183:110370.
[26] Xiao X, et al. Analytical model for the nonlinear buckling responses of the confined polyhedral FGP-GPLs lining subjected to crown point loading. Eng Struct 2023; 282:115780.
[27] Xiao X, et al. Nonlinear in-plane instability of the confined FGP arches with nanocomposites reinforcement under radially-directed uniform pressure. Eng Struct 2022;252:113670.
[28] Huang HY, Chang WS, Mosalam KM. Feasibility of shape memory alloy in a tuneable mass damper to reduce excessive in-service vibration. Struct Control Health Monit 2017;24(2):1–14.
[29] Nagarajaiah S, Varadarajan N. *Novel semiactive variable stiffness tuned mass damper with real time tuning capability*, t.E.M.C. Virginia.: ASCE; 2000.
[30] Sun C, et al. Hardening Duffing oscillator attenuation using a nonlinear TMD, a semi-active TMD and multiple TMD. J Sound Vib 2013;332(4):674–86.
[31] Aguiar RAA, Savi MA, Pacheco PMCL. Experimental investigation of vibration reduction using shape memory alloys. J Intel Mat Syst Str 2013;24(2):247–61.
[32] Mani Y, Senthilkumar M. Shape memory alloy-based adaptive-passive dynamic vibration absorber for vibration control in piping applications. J Vib Control 2015; 21(9):1838–47.
[33] Huang, H., W. Xie, and W.S. Chang, *Materials characterisation of NiTi and CuAlMn shape memory alloy bars under dynamic bending*, in *ASM International - International Conference on Shape Memory and Superelastic Technologies*. 2015, ASM International: Oxford, UK.
[34] Flemming L, Mascaro S. Analysis of hybrid electric/thermofluidic inputs for wet shape memory alloy actuators. Smart Mater Struct 2013;22(1):014015.
[35] Huang H. A Temperature Controlled Semi-active Tuned Mass Damper using Shape Memory Alloy for Vibration Reduction Applications. Department of Architecture and Civil Engineering. Bath, UK: University of Bath:; 2017.
[36] Huang HY, Zhu YZ, Chang WS. Comparison of Bending Fatigue of NiTi and CuAlMn Shape Memory Alloy Bars. Adv Mater Sci Eng 2020;2020.
[37] Zielinski TP, Duda K. Frequency and Damping Estimation Methods - an Overview. Metrology and Measurement Systems 2011;18(4):505–28.
[38] Zivanovic S, Pavia A. Probabilistic Assessment of Human Response to Footbridge Vibration. Journal of low frequency noise, vibration and active control 2009;28(4): 255–68.
[39] Shaw JA, Kyriakides S. Thermomechanical Aspects of Niti. J Mech Phys Solids 1995;43(8):1243–81.
[40] Fragiacomo M, Dujic B, Sustersic I. Elastic and ductile design of multi-storey crosslam massive wooden buildings under seismic actions. Eng Struct 2011;33(11): 3043–53.
[41] Blass, H.J. and P. Fellmoser, *Design of solid wood panels with cross layers*, in *8th World Conference on Timber Engineering* 2004: Lahti, Finland.
[42] Thompson SA. An overview of nickel-titanium alloys used in dentistry. Int Endod J 2000;33(4):297–310.
[43] Butaud P, Foltete E, Ouisse M. Sandwich structures with tunable damping properties: On the use of Shape Memory Polymer as viscoelastic core. Compos Struct 2016;153:401–8.
[44] Tsai H-C, Lin G-C. Optimum tuned-mass dampers for minimizing steady-state response of support-excited and damped systems. Earthq Eng Struct Dyn 1993;22 (11):957–73.
[45] Sadek F, et al. A method of estimating the parameters of tuned mass dampers for seismic applications. Earthq Eng Struct Dyn 1997;26(6):617–35.